

This article appeared in a journal published by Elsevier. The attached copy is furnished to the author for internal non-commercial research and education use, including for instruction at the authors institution and sharing with colleagues.

Other uses, including reproduction and distribution, or selling or licensing copies, or posting to personal, institutional or third party websites are prohibited.

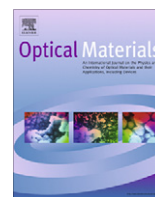
In most cases authors are permitted to post their version of the article (e.g. in Word or Tex form) to their personal website or institutional repository. Authors requiring further information regarding Elsevier's archiving and manuscript policies are encouraged to visit:

<http://www.elsevier.com/copyright>



Contents lists available at ScienceDirect

## Optical Materials

journal homepage: [www.elsevier.com/locate/optmat](http://www.elsevier.com/locate/optmat)First-principles study of the electronic structure and optical properties of the pure  $\text{BaY}_2\text{F}_8$ 

J.M. Dantas, M.V. Lalic\*

Universidade Federal de Sergipe, Departamento de Física, P.O. Box 353, 49100-000 São Cristóvão, SE, Brazil

## ARTICLE INFO

## Article history:

Received 25 January 2010

Received in revised form 2 May 2010

Accepted 6 May 2010

Available online 8 June 2010

## Keywords:

BYF

Dielectric tensor

Electronic structure

Optical absorption

## ABSTRACT

Ab-initio calculations based on density-functional theory have been employed to study the electronic structure and some optical properties of the pure  $\text{BaY}_2\text{F}_8$  (BYF) crystal. The band gap is calculated to be 7.5 eV. The electronic structure calculations revealed that the top of the valence band is dominated by the fluoride p-states, while the very bottom of the conduction band has predominantly yttrium d-character. The optical response in ultra-violet region is determined by calculating the complex dielectric tensor. It was found that the BYF crystal does not exhibit large optical anisotropy. Its principal absorption occurs due to electronic transitions from populated 2p states of the F to empty d-states of neighboring Y and Ba atoms.

© 2010 Elsevier B.V. All rights reserved.

## 1. Introduction

The fluoride compounds form an important class of materials that show peculiar chemical and physical characteristics: low refraction index, low phonon energy and wide-in-wavelength transmission region [1]. They are usually very attractive for optical applications because combine high quantum efficiency with favorable chemical and mechanical proprieties [2].

Barium yttrium fluoride,  $\text{BaY}_2\text{F}_8$  (BYF), is a material that provides a convenient crystalline matrix for effective upconversion processes thanks to its very low phonon energy ( $\hbar\omega \sim 350\text{--}380\text{ cm}^{-1}$  [3]). Owing to its good thermo-mechanical properties it is also investigated as active material for solid-state laser host [4]. Recently, the BYF doped with rare earth ions attracted attention due to its scintillation properties [5]. Despite considerable experimental effort to understand the mechanical and optical properties of the BYF, there is still a lack of theoretical knowledge of the compound, especially considering its band structure and absorption–emission characteristics.

The objective of this paper is to determine the electronic structure of the pure BYF crystal employing the state-of-art density-functional theory based calculations, and on this basis to analyze its optical absorption spectrum in the ultra-violet range (up to 40 eV). The interpretation of this spectrum in terms of band structure give insight into the manner by which the crystal respond to external electromagnetic perturbation. To the best knowledge of

authors, it is the first time that this kind of approach is applied to study the BYF system.

## 2. Calculations details and optimization of the crystal structure

The calculations were performed using the Full Potential Linear Augmented Plane Wave (FP-LAPW) method [6], the first-principles method based on density-functional theory (DFT) [7] and implemented in WIEN2k computer code [8]. In this method, the wave function and the potential are expanded in spherical harmonics inside non-overlapping spheres surrounding the atomic sites (muffin-tin spheres) and a plane wave basis set in the remaining space of the unit cell (interstitial region) is used. The muffin-tin radius  $R_{\text{MT}}$  was assumed to be 2.6, 2.0 and 1.5 au for Ba, Y and F, respectively. The valence wave functions inside the sphere are expanded up to  $l_{\text{max}} = 10$ . The plane wave cut off of  $K_{\text{max}} = 7.0/R_{\text{MT}}$  is chosen for the expansion of the wave functions in the interstitial region while the charge density was Fourier expanded up to  $G_{\text{max}} = 12$ . For k-space integration a mesh of 18 k-points in the irreducible part of the Brillouin zone was used. Exchange and correlation effects were treated by generalized-gradient approximation (GGA96) [9]. The  $^{56}\text{Ba}$ :  $5s^2 5p^6 6s^{12}$ ,  $^{39}\text{Y}$ :  $4s^2 4p^6 4d^1 5s^2$  and  $^9\text{F}$ :  $2s^2 2p^5$  electronic states were considered as valence ones, treated self-consistently within the scalar-relativistic approach, whereas the core states were relaxed in a fully relativistic manner.

The BYF crystallizes in a monoclinic structure with the C2/m space group [10]. The reticular constants are  $a = 0.6982\text{ nm}$ ,  $b = 1.0519\text{ nm}$ ,  $c = 0.4264\text{ nm}$ , with angle  $\gamma$  between the  $a$ -axis and the  $c$ -axis of  $99.7^\circ$ . The primitive unit cell contains two

\* Corresponding author. Tel.: +55 79 2105 6809; fax: +55 79 2105 6807.

E-mail addresses: [mlalic@ufs.br](mailto:mlalic@ufs.br), [mlalic@fisica.ufs.br](mailto:mlalic@fisica.ufs.br) (M.V. Lalic).

molecules of BaY<sub>2</sub>F<sub>8</sub>, i.e. 22 atoms. However, the WIEN2k package does not accept this description of the BYF structure due to the fact that some Wyckoff atomic positions are semi-populated. For this reason, the BYF crystal is represented by the triclinic structure with the space group P-1 (transformation from the C2/m to the P-1 structure was executed by PowderCell software [11]). In the light of new description, the lattice parameters are  $a = b = 0.6313$  nm and  $c = 0.4264$  nm, with angle  $\alpha = \beta = 95.33^\circ$  and  $\gamma = 112.84^\circ$ . The primitive unit cell contains one molecule of BYF, i.e. 11 atoms, from which the five are crystallographically inequivalent: the Ba, the Y, and the three types of the F: F<sub>1</sub>, F<sub>2</sub> and F<sub>3</sub>.

The BYF crystal structure was computationally optimized by permitting all the atoms inside the unit cell to move until the equilibrium is reached, in which the forces sensed by each atom are less than 3 mRy/au. Resultant theoretical structure is, however, found to be practically identical to the one experimentally determined, published in the Ref. [12]. This fact is presented in Table 1 which compares some selected inter-atomic distances in the BYF (first coordination spheres of the Ba and Y atoms).

### 3. Electronic structure

The calculated total density of states (TDOS) of the BYF compound is shown in Fig. 1. The spectrum consists of series of very well separated bands, reflecting a strong ionic character of atomic bonds in the crystal. The relatively broad band (with the width of approximately 3 eV) at the very top of the valence region is dominated by the F-2p states, containing almost six electrons per atom. This fact shows that the F attracted one extra electron inside its atomic sphere owing to its high electro-negativity. The Ba-5p states are concentrated within one narrow band positioned at the energy of –8 eV, and the rest of populated states lie in the lower energy part of the TDOS spectrum, as demonstrated in Fig. 1. The first peak at the very bottom of the conduction region, whose width is approximately 1 eV, has predominantly Y-d character. The next band, which begins at 8.5 and terminates at approximately 12 eV, consists of various peaks and contains a mixture of the Y-4d and Ba-5d states. The high-intensity peak centred at 13 eV, whose width is about 2 eV, originates from empty 4f states of the Ba, while the rest of the conduction band at higher energies consists of the hybridized states of the Ba, Y and F. The similar ordering and relative positions of Ba and F bands is reported for other fluoride compounds, such as BaLiF<sub>3</sub> [13]. The calculated value for the BYF band gap is 7.5 eV. Although we did not find any published experimental result for the BYF band gap, there exist indirect indications that it is much larger. The Ref. [14] reports the excitation spectrum of 5d → 4f emission of Er in BYF:Er, from which one can estimate absorption edge of the host at approximately 10–11 eV. This indication is confirmed in the Ref. [15] which study absorption of Dy in BYF:Dy up to energy of approximately 10 eV, at which seems to begin the host absorption. Discrepancy between calculated and experimental gap should be

attributed to the well known deficiency of the GGA to accurately describe electronic correlations.

### 4. Optical properties

The information about the optical response of solid materials can be accessed from the knowledge of their complex dielectric tensor  $\epsilon$ . The imaginary part of this tensor is directly proportional to the intensity of optical absorption and can be determined by computing the electric dipole matrix elements between the occupied and unoccupied electronic states. In the limit of linear optics, neglecting electron polarization effects and within the frame of random phase approximation, the expression for the imaginary part of  $\epsilon$  is the following [16]:

$$\text{Im}\epsilon_{\alpha\beta}(\omega) = \frac{4\pi^2 e^2}{m^2 \omega^2} \sum_{i,f} \int_{\text{BZ}} \frac{2dk}{(2\pi)^3} |\langle \varphi_{fk} | P_\beta | \varphi_{ik} \rangle| |\langle \varphi_{fk} | P_\alpha | \varphi_{ik} \rangle| \cdot \delta(E_f(k) - E_i(k) - \hbar\omega) \quad (1)$$

for a vertical inter-band transition from a filled initial state  $|\varphi_{ik}\rangle$  of energy  $E_i(k)$  to an empty final state  $|\varphi_{fk}\rangle$  of energy  $E_f(k)$  with the same wave vector  $k$ .  $\omega$  is the frequency of the incident radiation,  $m$  the electron mass,  $P$  the momentum operator, and  $\alpha$  and  $\beta$  stand for the projections  $x$ ,  $y$ ,  $z$ .

In the case of anisotropic material,  $\epsilon_{\alpha\beta}$  is a complex, symmetric, third-order tensor whose number of independent non-zero components depends on the crystal symmetry. As the BYF has the lowest, triclinic symmetry, its dielectric tensor has six independent components:  $\epsilon_{xx}$ ,  $\epsilon_{yy}$ ,  $\epsilon_{zz}$ ,  $\epsilon_{xy}$ ,  $\epsilon_{xz}$  e  $\epsilon_{yz}$ . We calculated imaginary part of all of them using the formula (1) for the range of incident radiation energies from 0 to  $\hbar\omega = 40$  eV. The real part of dielectric tensor is then determined using Kramers–Kronig relations. Both real and imaginary parts of  $\epsilon$  were calculated with a mesh of 221k-points in the irreducible wedge of the first Brillouin zone.

Every symmetric tensor can be reduced to its diagonal form by transforming the Cartesian coordinate system  $\{x, y, z\}$  in which it has been presented to another orthogonal system  $\{x', y', z'\}$ , usually called the principal axis system. We diagonalized the dielectric tensor of the BYF by resolving the eigenvalue problem:

$$\det(\text{Im}\epsilon_{ij} - \lambda I) = 0 \quad (2)$$

which is reduced to polynomial expression of the third degree in  $\lambda$ :

$$a\lambda^3 + b\lambda^2 + c\lambda + d = 0 \quad (3)$$

where

$$\begin{aligned} a &= -1 \\ b &= \text{Im}\epsilon_{xx} + \text{Im}\epsilon_{yy} + \text{Im}\epsilon_{zz} \\ c &= (\text{Im}\epsilon_{xy})^2 + (\text{Im}\epsilon_{xz})^2 + (\text{Im}\epsilon_{yz})^2 - \text{Im}\epsilon_{xx} \cdot \text{Im}\epsilon_{yy} - \text{Im}\epsilon_{xx} \cdot \text{Im}\epsilon_{zz} - \text{Im}\epsilon_{yy} \cdot \text{Im}\epsilon_{zz} \\ d &= 2 \cdot \text{Im}\epsilon_{xy} \cdot \text{Im}\epsilon_{xz} \cdot \text{Im}\epsilon_{yz} + \text{Im}\epsilon_{xx} \cdot \text{Im}\epsilon_{yy} \cdot \text{Im}\epsilon_{zz} - \text{Im}\epsilon_{xx} \cdot (\text{Im}\epsilon_{yz})^2 \\ &\quad - \text{Im}\epsilon_{yy} \cdot (\text{Im}\epsilon_{xz})^2 - \text{Im}\epsilon_{zz} \cdot (\text{Im}\epsilon_{xy})^2 \end{aligned}$$

**Table 1**

Selected Ba–F and Y–F inter-atomic distances in the BYF crystal, as calculated by the FP-LAPW method and compared with experimental data [12].

| Nearest-neighbor distance                    | Theory | Experiment | Nearest-neighbor distance | Theory | Experiment |
|--|--------|------------|---------------------------|--------|------------|
| <i>Inter-atomic distances in the BYF (Å)</i> |        |            |                           |        |            |
| Ba–F <sub>3</sub>                            | 2.714  | 2.715      | Y–F <sub>3</sub>          | 2.241  | 2.242      |
|  | 2.714  | 2.717      |                           | 2.241  | 2.226      |
| Ba–F <sub>2</sub>                            | 2.737  | 2.737      | Y–F <sub>2</sub>          | 2.259  | 2.259      |
|  | 2.737  | 2.738      |                           | 2.259  | 2.258      |
| Ba–F <sub>1</sub>                            | 2.859  | 2.859      | Y–F <sub>1</sub>          | 2.276  | 2.275      |
|  | 2.859  | 2.861      |                           | 2.276  | 2.276      |
| Ba–F <sub>1</sub>                            | 2.929  | 2.929      | Y–F <sub>1</sub>          | 2.326  | 2.326      |
|  | 2.929  | 2.928      |                           | 2.326  | 2.326      |

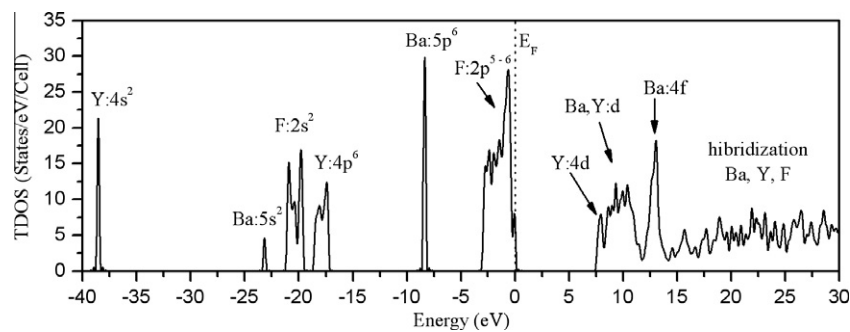


**Fig. 1.** Calculated total DOS of the  $\text{BaY}_2\text{F}_8$ . The dominant orbital characters of the bands are indicated. Dashed line denotes Fermi level.

The eigenvalues ( $\lambda_1, \lambda_2, \lambda_3$ ) are expressed in terms of the calculated  $\text{Im}(\epsilon_{ij})$  with the aid of the software Math Cad, but these expressions are not presented here due to their very long and complex form. As a result, we determined the three components of the BYF dielectric tensor along its principal optical axes. Their imaginary parts, proportional to the optical absorption spectrum of the BYF, are presented in Fig. 2.

From Fig. 2 it can be seen that the absorption curves have very similar form along the three principal axes, with the main peaks

centred on the same energy values. Thus, we conclude that the BYF crystal does not exhibit large optical anisotropy. It mostly absorbs the light whose energy lies within the energy interval of the first absorption peak, with theoretical limits from 7.5 to 12.5 eV. Due to underestimation of the theoretical gap value, however, the limits of this interval should be shifted to 3–4 eV higher energies.

With the objective to analyze the manner by which the BYF absorbs the incident radiation, we interpreted its absorption spectra

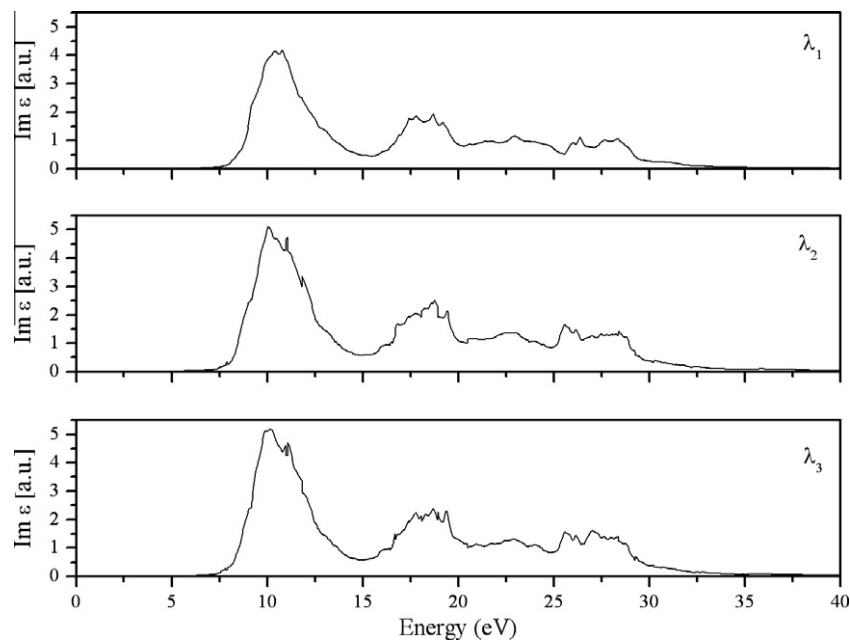


**Fig. 2.** Imaginary part of the dielectric tensor of the pure BYF crystal calculated along its principal optical axes and expressed as function of the incident radiation energy.

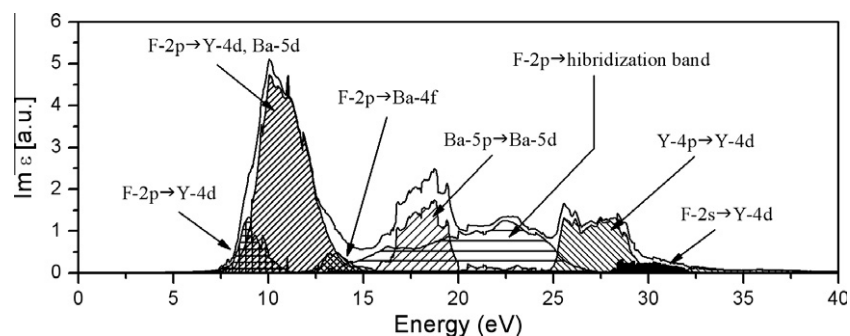


**Fig. 3.** Imaginary part of the dielectric tensor  $\lambda_2$  of the pure BYF crystal interpreted in terms of inter-band electronic transitions.

in terms of the electronic structure shown in Fig. 1. As the absorption curves are similar, we choose one of them (actually  $\lambda_2$ ) as the representative, and presented its decomposition in terms of electronic inter-band transitions in Fig. 3.

The first, lowest energy peak, originates from the electron transfer from the very top of the valence band to the very bottom of the conduction band. It is thus dominated by the electronic transitions from the full F-2p states to the empty d-states of neighboring Ba and Y ions. The transitions from the F-2p to the Ba-4f states contribute very little to overall absorption. The second peak, positioned between 15 and 20 eV, originates from two contributions: (1) the transitions from the Ba-5p to the Ba-5d states, and (2) the transitions from the F-2p states to the empty states at higher energy (hybridization band in Fig. 1). The last type of transitions is responsible for the formation of the next structure in the absorption spectrum, situated between 20 and 25 eV. The radiation with the energy between 25 and 29 eV is absorbed via Y-4p to Y-4d electron transition, while the transitions from the F-2s to the Y-4d states dominate the highest energy part of the absorption spectrum, yet characterized with low intensity. Again, all energy intervals reported above should be shifted about 3–4 eV to higher values in order to match the experimental situation.

## 5. Conclusion

We employed the first-principles, DFT based, FP-LAPW method to study structural, electronic and optical properties of the pure BaY<sub>2</sub>F<sub>8</sub> (BYF) crystal. It was found that the calculated atomic positions within the BYF unit cell agree very well with the published experimental data. The calculated electronic structure revealed the orbital character of the most important bands. The top of the valence band consists of the fluorine 2p states while the conduction band bottom is dominated by the Y and Ba d-states. The gap is calculated to be 7.5 eV, underestimated in relation to experi-

ment. The optical absorption of the BYF in the ultra-violet region was analyzed by calculating its dielectric tensor. It was concluded that BYF does not exhibit large optical anisotropy. Its absorption spectrum is interpreted in terms of inter-band electronic transitions. The analysis showed that the BYF absorbs mostly in the energy region that corresponds to the lowest energy absorption band owing to transitions from the F-2p states to the Y and Ba d-states.

## Acknowledgements

The authors gratefully acknowledge the CNPq and FAPITEC-SE (Brazilian funding agencies) for financial support.

## References

- [1] J.C. Wright, Radiationless processes in molecules and condensed phases, in: F.K. Fong (Ed.), Topics in Applied Physics, Springer, Berlin, 1976.
- [2] M. Karbowiak, A. Mech, A. Bednarkiewicz, W. Strek, J. Lumin. 114 (2005) 1.
- [3] E.B. Sveshnikova, A.A. Stroganov, N.T. Timofeev, Opt. Spectrosc. 64 (1993) 73.
- [4] V. Toccafondo et al., J. Appl. Phys. 101 (2007) 023104.
- [5] J.C. van't Spijker et al., J. Lumin. 85 (1999) 11.
- [6] O.K. Andersen, Phys. Rev. B 12 (1975) 3060; D.J. Singh, Plane Waves, Pseudopotentials and the LAPW Method, Kluwer Academic, Dordrecht, 1994.
- [7] P. Hohenberg, W. Kohn, Phys. Rev. 136 (1964) B864; W. Kohn, L.J. Sham, Phys. Rev. 140 (1965) A1133.
- [8] P. Blaha, K. Schwarz, G.K.H. Madsen, D. Kvasnicka, J. Luitz, An Augmented Plane Waves + Local Orbital Program for Calculating Crystal Properties, Institut Für Physikalische und Theoretische Chemie, Wien, Austria, 2001.
- [9] J.P. Perdew, S. Burke, M. Ernzerhof, Phys. Rev. Lett. 77 (1996) 3865.
- [10] O.E. Izotova, V.B. Aleksandrov, Dokl. Akad. Nauk USSR 192 (1970) 1037.
- [11] <<http://www.ccp14.ac.uk/tutorial/powdcell/index.html>>.
- [12] L.H. Guilbert et al., Mater. Res. Bull. 28 (1993) 923.
- [13] S. Amara Korba, H. Meradji, S. Ghemid, B. Bouhafs, Comput. Mater. Sci. 44 (2009) 1265.
- [14] J. Becker et al., J. Alloys Compd. 275–277 (1998) 205.
- [15] V.V. Apollonov, A.A. Pushkar, T.V. Uvarova, S.P. Chernov, Phys. Solid State 50 (2008) 1660.
- [16] M. Bass, E.W.V. Stryland, D.R. Williams, W.L. Wolfe, Handbook of Optics, vol. 1, second ed., McGraw-Hill, New York, 1995.